Cerenkov second-harmonic arc from a hexagonally poled $LiTaO_3$ planar waveguide

2009 J. Phys. D: Appl. Phys. 42 215103

(http://iopscience.iop.org/0022-3727/42/21/215103)

J. Phys. D: Appl. Phys. **42** (2009) 215103 (4pp) doi:10.1088/0022-3727/42/21/215103

Cerenkov second-harmonic arc from a hexagonally poled $LiTaO_3$ planar waveguide

Yong Zhang[1,2,3], X P Hu[1], G Zhao[1], S N Zhu[1,3] and Min Xiao[1,2]

[1] National Laboratory of Solid State Microstructures, Nanjing University, Nanjing, 210093, People's Republic of China
[2] Department of Physics, University of Arkansas, Fayetteville, AR 72701, USA

E-mail: yong_zhang_@163.com and zhusn@nju.edu.cn

Received 7 July 2009, in final form 28 August 2009
Published 13 October 2009
Online at stacks.iop.org/JPhysD/42/215103

Abstract
We demonstrate a new type of arc-shaped Cerenkov second-harmonic generation in a hexagonally poled $LiTaO_3$ planar optical waveguide. Scattering of fundamental light, arising from domain walls and other imperfections on the surface and inside the waveguide, is found to be involved in such an optical parametric process, which is enhanced in the modulated domain structure by quasi-phase matching. One can use the Cerenkov second-harmonic arc to study the structure information of a nonlinear optical waveguide and to characterize the scattering in the waveguide.

(Some figures in this article are in colour only in the electronic version)

1. Introduction

Recently, nonlinear Cerenkov radiation (NCR) associated with a $\chi^{(2)}$ nonlinear optical process has attracted increasing interest [1–10]. In the Cerenkov configuration, a coherent harmonic wave at a new frequency will be emitted along the direction of the Cerenkov angle when the nonlinear polarization, driven by incident light field, has a faster phase velocity than that of the harmonic wave in the medium. It is relatively simple for Cerenkov second-harmonic generation (SHG). In this case, the radiation source (i.e. nonlinear polarization) and the incident light have the same phase velocity. Cerenkov angle θ_c is defined by

$$\theta_c = \arccos(\upsilon'/\upsilon), \quad (1)$$

where υ and υ' are the phase velocities of the fundamental and SH waves, respectively. Cerenkov SHG occurs when $\upsilon > \upsilon'$. Compared with the conventional $\chi^{(2)}$ process, NCR can only be realized in a thin nonlinear crystal using a short-pulsed laser (less than several nanoseconds) [1, 2], in fibre [3] or in waveguide [4–8]. The generated harmonic radiation may present a ring-shaped pattern from the crystal or the fibre [1–3], or form a well-collimated beam from a planar waveguide [4–8].

The quasi-phase-matching (QPM) [11] technique has been widely used in frequency-conversion [11–14] and quantum information [15–17]. It can also be used to realize the modulation of NCR. Recently, we reported QPM Cerenkov SHG [9] and sum-frequency generation (SFG) [10] in a nonlinear photonic crystal [18] waveguide. QPM can provide an additional phase by modulating the nonlinear susceptibility tensor of the nonlinear crystal, then change the phase velocity of the nonlinear polarization, therefore, and lead NCRs to be radiated along different directions. In this paper, we report a novel Cerenkov process, Cerenkov second-harmonic (SH) arc, generated from a hexagonally poled $LiTaO_3$ waveguide. The SH arc will emerge when a z-polarized fundamental wave is focused into the nonlinear crystal waveguide. The arc projected onto the screen behind the sample is always accompanying a Cerenkov SHG spot. Further study shows that the arc is related to a scattering-involved Cerenkov SHG process. The structure information of the domain structure and the spatial distribution of the scattering signal are recorded in the SH arc pattern.

[3] Authors to whom any correspondence should be addressed.

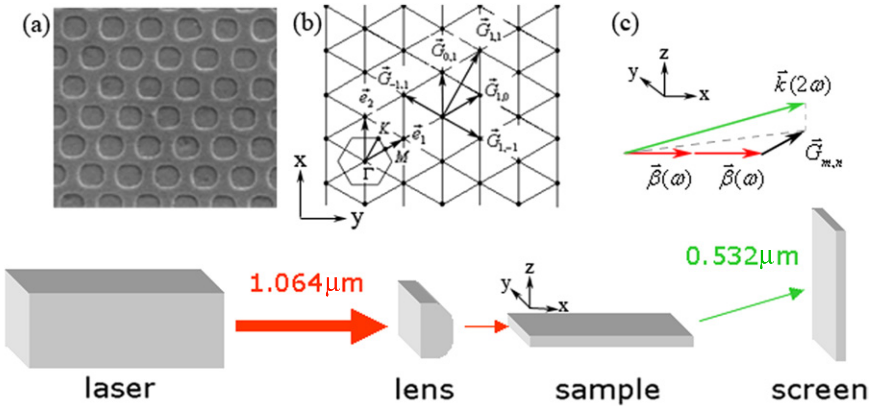

Figure 1. Experimental setup. The insets are (*a*) domain structure of the sample used, (*b*) the corresponding reciprocal lattice vectors and (*c*) the phase-matching geometry for QPM Cerenkov SHG.

2. Experimental setup

In the experiment, the sample is a hexagonally poled $LiTaO_3$ with a domain interval of $a = 9.0\,\mu$m (figure 1(*a*)) fabricated at room temperature by an electric-field-poling technique [19]. This structure can provide reciprocal lattice vectors with six-fold symmetry defined by $\vec{G}_{m,n} = (4\pi/\sqrt{3}a)(m^2+n^2+m\cdot n)^{1/2}$ with m and n being indices of reciprocal vectors (figure 1(*b*)) [18]. Then a planar high-refractive-index (n_e) layer was fabricated on top of the poled sample through a proton-exchange procedure. Subsequently, the sample was subjected to annealing treatment in a tube furnace, which recovered the nonlinear coefficient and created a graded-index waveguide layer with a larger thickness [20]. The propagation constant of the fundamental mode at 1.064 μm in the waveguide is measured to be 12.68 μm^{-1}.

Figure 1 shows the experimental setup. The laser is a diode-pumped, Q-switched Nd : YAG laser, providing a z-polarized fundamental beam at 1.064 μm. The pulse width is 90 ns and the repetition rate is 8 kHz. The fundamental beam is coupled into the planar waveguide by a cylindrical lens and propagates along the x-axis of the crystal. The generated SH wave is projected onto a screen placed 15 cm away from the end face of the sample. A band-pass filter is used to filter out the fundamental beam and no focusing lens is used after the output end face. The operating temperature is kept at 25 °C.

3. Experimental results and discussion

When a 1.5 W fundamental beam is coupled into the waveguide, the SH radiation pattern projected onto the screen is shown in figure 2(*a*). In this picture, three vertical lines at the bottom of the picture and nine spots tangled with arcs composed a green 'tree'. The lines correspond to the guided-to-guided QPM SHG processes [21], but they are not perfectly phase matched at the experimental operating temperature. All the spots on the screen are from Cerenkov SHG. They distribute with a mirror symmetry as shown in figure 2(*a*). As discussed in [9, 10], the reciprocal vector provided by the 2D hexagonal lattice leads the radiation to propagate along different directions and results in the tree-shaped pattern on the screen. The phase-matching condition for Cerenkov SHG can be written in wave vector space as [9]

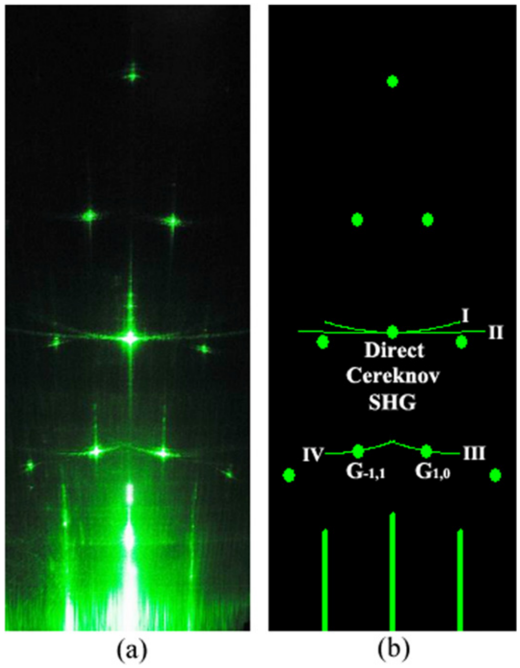

Figure 2. The experimental SH pattern projected onto the screen (*a*) and the calculated pattern (*b*).

$$\left|2\vec{\beta}\,(\omega) + \vec{G}_{m,n}\right| = \left|\vec{k}\,(2\omega)\right| \cos\theta_c, \qquad (2)$$

where $\vec{\beta}(\omega)$ and $\vec{k}(2\omega)$ are the wave vectors of the guided fundamental wave in the waveguide and the radiated SH wave along the Cerenkov angle θ_c in the substrate, respectively. The corresponding phase-matching geometry is shown in figure 1(*c*). In figure 2(*a*), three spots are much brighter than the others, the spot at the centre of the picture is from a direct Cerenkov SHG process in which no reciprocal vector is involved and two spots located at lower positions correspond to noncollinear reciprocal lattice vectors $G_{1,0}$ and $G_{-1,1}$, respectively. Details are presented in [9, 10]

On careful examination of figure 2(*a*) one can find that the SH arcs are around all Cerenkov spots. In particular

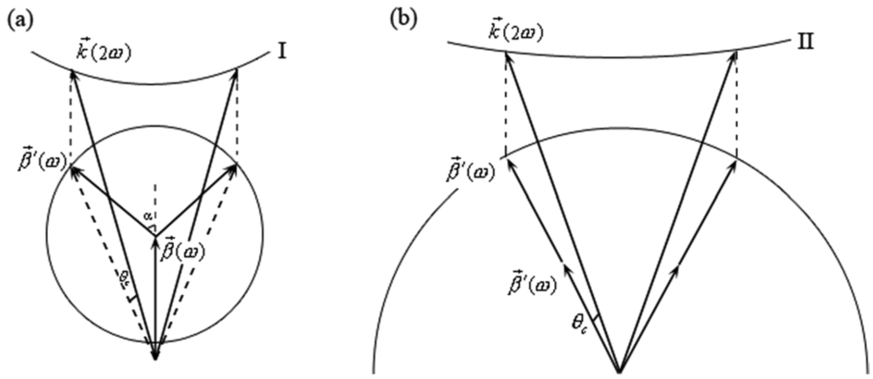

Figure 3. The scattering-involved phase-matching geometry for Cerenkov SH arcs labelled as I (*a*) and II (*b*) shown in figure 2.

for the brightest centre one, two clear arcs with different curvatures can be observed. This SH arc phenomenon results from another type of nonlinear interaction, i.e. a scattering-involved Cerenkov SHG. When the fundamental wave passes through the waveguide, the elastic scattering could take place at the domain walls and other defects on the surface and inside the waveguide and does not change the wavelength of the light [22]. In a nonlinear medium, the scattered light can fulfil SHG with the incident fundamental wave and this process can be greatly enhanced in QPM structures.

Let us first consider the two SH arcs around the centre spot. Since no reciprocal vector participates, the phase-matching condition for this Cerenkov spot is

$$\left|2\vec{\beta}(\omega)\right| = \left|\vec{k}(2\omega)\right| \cos\theta_c. \tag{3}$$

When a scattered fundamental wave $\vec{\beta}'(\omega)$ is introduced, the corresponding phase-matching condition can be rewritten as

$$\left|\vec{\beta}(\omega) + \vec{\beta}'(\omega)\right| = \left|\vec{k}(2\omega)\right| \cos\theta_c. \tag{4}$$

In the experiment, the scattered light $\vec{\beta}'(\omega)$ exists mainly in the x–y plane due to the confinement of the planar waveguide. $\vec{\beta}'(\omega)$ presents a continuous and symmetrical spatial distribution from $\vec{\beta}(\omega)$ [22]. The phase-matching geometry is shown in figure 3(*a*). In this process, the scattered wave $\vec{\beta}'(\omega)$ and the incident wave $\vec{\beta}(\omega)$ generate a nonlinear polarization at the frequency of 2ω, which then emits coherent SH wave to the substrate under the Cerenkov configuration. Because of the symmetric distribution of the scattered light, the generated SH radiation also has a mirror symmetry. The calculated result is the arc labelled as I shown in figure 2(*b*), which is very consistent with the arc of bigger curvature in figure 2(*a*). The other arc can also be deduced in terms of (3) in which two collinearly scattered fundamental waves are introduced. The corresponding phase-matching condition is expressed as

$$\left|2\vec{\beta}'(\omega)\right| = \left|\vec{k}(2\omega)\right| \cos\theta_c. \tag{5}$$

This equation is very similar to (3), except that now $\vec{\beta}'(\omega)$ replaces $\vec{\beta}(\omega)$. The corresponding geometry is shown in figure 3(*b*). The calculated result is labelled as II shown in figure 2(*b*). Moreover, there is another possibility; two noncollinearly scattered fundamental waves are involved in the Cerenkov SHG. This type of NCR is too weak to be observed in this experiment because of the limited interacting length between the interactional waves. It should be mentioned that the $LiTaO_3$ crystal has birefringence. However, the birefringence of the crystal is very small [23], and, therefore, is negligible in our calculations.

When a reciprocal vector is involved, the situation is quite similar to the cases as discussed above. The phase-matching condition with one scattered fundamental wave can be written as

$$\left|\vec{\beta}(\omega) + \vec{\beta}'(\omega) + \vec{G}_{m,n}\right| = \left|\vec{k}(2\omega)\right| \cos\theta_c. \tag{6}$$

The scattered wave $\vec{\beta}'(\omega)$ and the incident wave $\vec{\beta}(\omega)$ still generate a nonlinear polarization at the frequency of 2ω at first. However, the phase velocity of the nonlinear polarization is changed by $\vec{G}_{m,n}$ [9, 10], which leads to the tilt and distortion of the Cerenkov SH arc compared with the previous one without reciprocal vectors involved when projected onto the screen. In our calculation, we analysed the Cerenkov SH arcs associated with noncollinear reciprocal vectors $G_{1,0}$ and $G_{-1,1}$. The phase-matching geometry is shown in figure 4 and the calculated results are the arcs labelled as III and IV shown in figure 2(*b*). The theoretical calculations are very consistent with the experimental patterns. Here, nonlinear optical processes involving two scattered fundamental waves could not be presented because of low intensities.

The intensity of the SH arc strongly depends on the distribution of the scattering light in the waveguide. By solving the nonlinear wave equation, the Cerenkov SH intensity can be expressed as $I(2\omega) \propto I(\omega)I'(\omega)L^2$, where $I(\omega)$ is the intensity of the fundamental wave, $I'(\omega)$ the scattering intensity and L the interaction length. Considering the arc labelled as I in figure 2(*a*), the SHG intensity is the strongest at the corresponding Cerenkov spot, and then decreases considerably along the arc when moving outwards. With simple calculations, we can deduce that a strong scattering occurs when $\alpha < 5^\circ$, where α is the angle between $\vec{\beta}'(\omega)$ and $\vec{\beta}(\omega)$ as shown in figure 3(*a*).

Scattering is one of the basic processes when light travels through matter. It originates from the optical inhomogeneity of

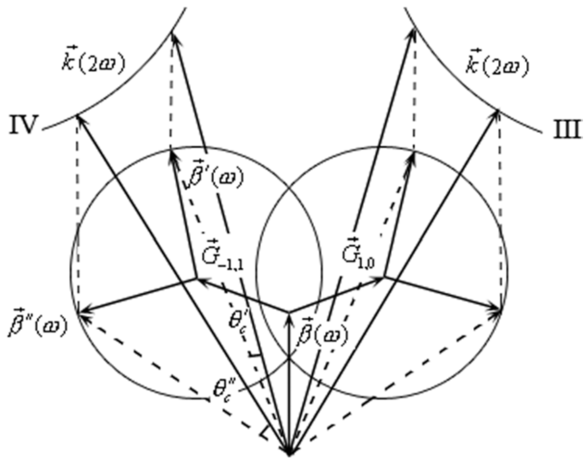

Figure 4. The phase-matching geometry of QPM Cerenkov SH arcs labelled as III and IV shown in figure 2. $\vec{\beta}'(\omega)$ and $\vec{\beta}''(\omega)$ represent scattered fundamental light.

the material, including fluctuation of the refractive index and defects inside the matter. Now, nonlinear optical interactions, such as spontaneous noncollinear frequency doubling in a photorefractive crystal [24], conical SHG in a periodically poled ferroelectric material [22] and so on, have become important methods for studying scattering in nonlinear bulk crystals. Now, the Cerenkov SH arc provides a new method for evaluating scattering in a nonlinear waveguide. Since the phase-matching condition under the Cerenkov configuration is automatically satisfied [4–6], such a Cerenkov SH arc is usually more efficient in converting the scattered light. Also, it has wide phase-matching bandwidth [5] and large tolerance of variations in pump wavelength and waveguide parameters. These advantages make the Cerenkov arc a good tool for the characterization of nonlinear waveguides.

4. Conclusion

We studied Cerenkov SH arcs from a hexagonally poled $LiTaO_3$ planar waveguide. Theoretical analyses show that nonlinear optical processes under the Cerenkov configuration involving scattering inside the waveguide are responsible for this phenomenon. The distribution of such an arc-shaped pattern projected onto the screen is related to the spatial symmetry of the scattered fundamental light and the domain structure.

Acknowledgments

This work is supported by the China Postdoctoral Science Foundation funded project 20070420992, Jiangsu Planned Projects for Postdoctoral Research Funds 0702016B and the National Natural Science Foundation of China (No 10534020).

References

[1] Fragemann A, Pasiskevicius V and Laurell F 2004 *Appl. Phys. Lett.* **85** 375
[2] Vaicaitis V 2002 *Opt. Commun.* **209** 485
[3] Chikuma K, Okamoto S, Uenishi N, Uemiya T and Umegaki S 2004 *Appl. Opt.* **43** 4697
[4] Yamamoto H and Sugiyama T 1997 *J. Opt. Soc. Am.* B **14** 1831
[5] Wang G Y, Yang Y and Garmire E 1995 *Appl. Phys. Lett.* **66** 3416
[6] Schmitt K, Benecke C and Schadt M 1997 *J. Appl. Phys.* **81** 11
[7] Pezzetta D, Sibilia C and Bertolotti M 2002 *J. Opt. Soc. Am.* B **19** 2102
[8] Wang F, Cao Z and Shen Q 2005 *Opt. Lett.* **30** 522
[9] Zhang Y, Qi Z, Wang W and Zhu S N 2006 *Appl. Phys. Lett.* **89** 171113
[10] Zhang Y, Gao Z D, Qi Z, Zhu S N and Ming N B 2008 *Phys. Rev. Lett.* **100** 163904
[11] Zhu S N, Zhu Y Y and Ming N B 1997 *Science* **278** 843
[12] Xu P, Wang J F, Li C, Xie Z D, Lv X J, Leng H Y, Zhao J S and Zhu S N 2009 *Opt. Express* **17** 4289
[13] Liu H C and Kung A H 2008 *Opt. Express* **16** 9714
[14] Peng L H, Hsu C C, Ng J and Kung A H 2004 *Appl. Phys. Lett.* **84** 3250
[15] Yu X Q, Xu P, Xie Z D, Wang J F, Leng H Y, Zhao J S, Zhu S N and Ming N B 2008 *Phys. Rev. Lett.* **101** 233601
[16] Torres J P, Alexandrescu A, Carrasco S and Torner L 2004 *Opt. Lett.* **29** 376
[17] Yu Y B, Zhu S N, Yu X Q, Xu P, Wang J F, Xie Z D and Leng H Y 2008 *Phys. Rev.* A **77** 032317
[18] Berger V 1998 *Phys. Rev. Lett.* **81** 4136
[19] Zhu S N, Zhu Y Y, Zhang Z Y, Shu H, Wang H F, Hong J F, Ge C Z and Ming N B 1995 *J. Appl. Phys.* **77** 5481
[20] Suchosiki P G, Findakly T K and Leonberger F J 1988 *Opt. Lett.* **13** 1050
[21] Gallo K, Codemard C, Gawith C B, Nilsson J, Smith P G R, Broderick N G R and Richardson D J 2006 *Opt. Lett.* **31** 1232
[22] Xu P, Ji S H, Zhu S N, Yu X Q, Sun J, Wang H T, He J L, Zhu Y Y and Ming N B 2004 *Phys. Rev. Lett.* **93** 133904
[23] Abedin K S and Ito H 1996 *J. Appl. Phys.* **80** 6561
[24] Kasemir K U and Betzler K 1999 *Appl. Phys.* B **68** 763